Technical Report

A histopathological analysis of spontaneous neoplastic and non-neoplastic lesions in aged male RccHan:WIST rats

Motoki Hojo[1]*, Yoshimitsu Sakamoto[1], Ai Maeno[1], Kuniaki Tayama[1], Yukie Tada[1], Katsuhiro Yuzawa[1], Hiroshi Ando[1], Yoshikazu Kubo[1], Akemichi Nagasawa[1], Kazuyoshi Tanaka[1], Norio Yano[1], Fujifumi Kaihoko[1], Yuko Hasegawa[1], Toshinari Suzuki[1], Akiko Inomata[1], Takako Moriyasu[1], Katsuhiro Miyajima[2], and Dai Nakae[2]*

[1] Department of Pharmaceutical and Environmental Sciences, Tokyo Metropolitan Institute of Public Health, 3-24-1 Hyakunincho, Shinjuku, Tokyo 169-0073, Japan

[2] Department of Nutritional Science and Food Safety, Faculty of Applied Biosciences, Tokyo University of Agriculture, 1-1-1 Sakura-ga-Oka, Setagaya, Tokyo 156-8502, Japan

Abstract: Histopathological information about spontaneous lesions in aged Hannover Wistar rats is limited. In this study, we describe spontaneous lesions found in 39 male RccHan:WIST rats used as a control in a carcinogenicity study. Neoplastic lesions were frequently seen in the endocrine system, such as pituitary adenomas in the pars distalis. This strain exhibited a high incidence of thymoma (10.3%), compared to other strains. We encountered an oligodendroglioma, a pituitary adenoma of the pars intermedia, and a prostate adenocarcinoma, which are comparatively rare in rats. While the variety and incidence of non-neoplastic lesions were similar to those in other strains, several interesting lesions occurred with relatively high incidence, including "harderianization" of the extraorbital lacrimal gland, common bile duct ectasia, and hyperplasia of pulmonary endocrine cells in the lung. Furthermore, comparative analyses demonstrated that the severity of chronic progressive nephropathy and murine progressive cardiomyopathy in RccHan:WIST rats was less than that in F344 rats. (DOI: 10.1293/tox.2019-0064; J Toxicol Pathol 2020; 33: 47–55)

Key words: RccHan:WIST, spontaneous lesion, aged-rat, strain-difference, non-neoplastic lesion

Hannover Wistar rats are widely used for long-term toxicological and carcinogenic studies because they possess a number of advantageous characteristics, including a higher survival rate, a smaller size, and lower incidences of tumors, compared to those of other strains such as the Sprague-Dawley (SD) rats. RccHan:WIST, a Wistar substrain, has been recently available in Europe, the US, and Japan. Envigo (Huntingdon, UK) has provided background data for this strain, showing that there are differences in the incidence or severity of some neoplasms or toxicologically important lesions[1, 2]. In Japan, several pathologists have reported on the characteristics and biochemical parameters of RccHan:WIST rats[3], as well as spontaneous lesions that have occurred in the cornea[4] and the uterine horn[5]. However, few reports have been published so far discussing a comprehensive analysis of spontaneous lesions in aged rats of this strain, especially non-neoplastic lesions. Only Blankenship *et al.* reported microscopic findings of various lesions seen in routine toxicological studies[6]. The present study highlights our experience with naturally occurring neoplastic and non-neoplastic lesions in 39 male RccHan:WIST rats at 2 years of age. In addition, some non-neoplastic lesions, such as chronic progressive nephropathy (CPN), were comparatively analyzed using our specimens from aged male Fischer 344 (F344) rats.

Male RccHan:WIST rats were obtained from Japan Laboratory Animals Inc. (Saitama, Japan). The rats were provided a basal diet, CR-LPF (Oriental Yeast Co. Ltd, Tokyo, Japan), and tap water *ad libitum*, and individually housed in hanging-wire stainless-steel mesh cages in a room maintained at a temperature of 24°C and 55% humidity on a 12-h light–dark cycle. Of the 20 rats used as vehicle control and 20 rats used as non-treated control for a carcinogenic study, 39 were histopathologically analyzed in this study. The remaining animal developed eating disorder symptoms due to a deformed cranial incisor tooth, and thus was excluded from the analysis. Rats belonging to the vehicle group were intratracheally instilled with saline containing 0.5% Tween 80 and 0.5% sucrose 12 times every 4 weeks from the age of 10 weeks to 54 weeks. Since there was no apparent difference in the types and incidences of histological findings between the two groups (data not

shown), these data were combined and described as a single data set. Necropsies were conducted whenever moribund or dead animals were found. All remaining animals were killed at 104–110 weeks of age. Thereafter, all tissues and tumor masses were excised, fixed in 10% neutrally buffered formalin, embedded in paraffin, sectioned, and stained with hematoxylin and eosin (HE). When a tissue sample was too autolytic or too small to allow histological analysis, it was excluded. For immunohistochemical staining, antigen retrieval was performed using a microwave for 10 min followed by inactivation of endogenous peroxidase. After blocking, the sections were treated with the following primary antibodies: oligodendrocyte lineage transcription factor-2 (Olig-2; IBL, Gunma, Japan: 18953, rabbit polyclonal), glial fibrillary acidic protein (GFAP; Abcam, Cambridge, UK: ab7260, rabbit polyclonal), α-melanocyte-stimulating hormone (α-MSH; Abcam: ab123811, rabbit polyclonal), adrenocorticotropic hormone (ACTH; Abcam: ab74976, rabbit polyclonal), cytokeratin 18 (PROGEN, Heidelberg, Germany: 61028, mouse monoclonal), protein G product 9.5 (PGP9.5; Abcam: ab8189, mouse monoclonal), Clara cell 16 kDa protein (CC16; Cloud-Clone, Houston, TX, USA: PAA857Ra01, rabbit polyclonal), and placental glutathione S-transferase (GST-P; MBL, Aichi, Japan: 311, rabbit polyclonal). Diaminobenzidine signals were detected with a horseradish peroxidase-secondary antibody conjugate (Agilent Technologies, Santa Clara, CA, USA: K4061).

For the comparative analysis of non-neoplastic lesions, another set of specimens was collected from 37 non-treated male F344/NJic rats at 2 years of age (obtained from Central Institute for Experimental Animals; Kanagawa, Japan). The number, area of GST-P positive foci of hepatocytes (consisting of more than five positive cells), and tissue section size were measured with an image analyzer, Image J (NIH; http://imagej.nih.gov/ij/download.html). CPN was classified into 8 grades corresponding to lesion progression[7]: Grade 0, no lesions; grade 1, minimal lesion; grade 2, mild lesion; grade 3, low-moderate; grade 4, mid-moderate; grade 5, high-moderate; grade 6, low-severe; grade 7, high-severe; and grade 8, end-stage. Murine progressive cardiomyopathy (PCM) was analyzed using HE staining and as well as Masson's trichrome staining, confirming fibrosis, and grading was defined as the extent of lesions in the heart sections as follows[8]: Grade 0, no or only minimal changes; grade 1, <10%; grade 2, 11–40%; grade 3, 41–80%; and grade 4, >81%. The incidence of pulmonary neuroendocrine cell (PNEC) hyperplasia was evaluated by searching the sections immunohistochemically stained with the anti-PGP9.5 antibody. For each animal, 4 sections (all the from right lobe of the lung) were examined. Statistical analyses were performed using a StatLight software (Yukms. Co. Ltd; Kanagawa, Japan). Analyses of GST-P positive foci of hepatocytes and the gradings of CPN and PCM were all evaluated using Mann Whitney's U-test. A comparison of incidence of PNEC was evaluated using Fisher's exact test. The difference of the values was deemed statistically significant when the p value was less than 0.05.

All animal experiments were approved by the Animal Experiment Committee of the Tokyo Metropolitan Institute of Public Health.

Thirty-three of the 39 rats were killed at 104–110 weeks of age as scheduled necropsy, while four dead animals and two moribund animals were necropsied before this stage. The four dead animals were found from 85 to 110 weeks of age, two of which died of severe compression of the brain due to a large adenoma of pituitary pars distalis, while the other two died of severe anemia due to a large granular lymphocyte leukemia (LGL) in one case and a large hemangioma in the subcutis in the other case. Of the two moribund rats, one succumbed to an oligodendroglioma, whereas the other suffered from an adenoma of the pituitary pars distalis, and they were euthanized at 28 and 91 weeks, respectively. The survival rate at 104 weeks was 87.2%, and the mean survival time was 100.7 weeks. Body weight plateaued at 12–14 weeks of age, and the mean body weight increased to a maximum of 532.9 ± 63 g at the age of 94 weeks. The mean body weight at death was 520.7 ± 69 g (range: 423.6 to 730.4).

Table 1 summarizes the numbers and incidences of neoplasms observed in this study. Among the 39 rats, 30 had some form of neoplasia (76.9%), and 14 had two or more types of tumors simultaneously (35.9%).

As for neoplasms of the brain, a granular cell tumor and an oligodendroglioma were observed. A large cohort analysis of RccHan:WIST rats showed that oligodendroglioma developed at an earlier age in these rats than did other brain tumors[9]. Likewise, a high-grade oligodendroglioma may have progressed aggressively and killed an adult rat at 28 weeks of age in our study; a large area of the right cerebral hemisphere appeared darkened and swollen. Histologically, a tumor involving a large hemorrhagic cyst at the center of the lesion compressed the normal brain tissue (Fig. 1A). Round tumor cells with chromatin-rich nuclei were arranged in rows, similar to the typical honeycomb structure (Fig. 1B and C). Neoplastic cells partially exhibited atypia and pleomorphism, accompanied by numerous irregularly shaped capillaries, eosinophilic extracellular substances, and necrosis (Fig. 1B). The tumor cells were immunohistochemically positive for a specific oligodendrocyte marker, Olig-2 (Fig. 1D), while they were almost all negative for a glial cell marker, GFAP (Fig. 1D inset).

A greater incidence of thymoma in Hannover Wistar rats has been reported as one of the characteristics of this strain[2,6]. Consistent with this, four thymomas occurred in this study (10.3%). One tumor showed a marked expansion with compression of unaffected tissue, and its histological structure resembled normal thymic architecture consisting of cortex-like (lymphocyte-rich) and medulla-like (epithelial cell-rich) areas (Fig. 1E and F) as previously reported[10]. Neoplastic cells were immunohistochemically positive for cytokeratin 18 (Fig. 1G). LGL was found in two dead animals, both of which showed splenomegaly and metastases in the lung and liver.

The endocrine system had the highest number of tu-

Table 1. Spontaneous Neoplasms Observed in Aged RccHan:WIST Male Rats

Organ system		Neoplasm	No. of rats with tumors	Rate (%)
Nervous system	Brain	Tumor, granular cell, benign	1	2.6
		Oligodendroglioma, malignant, high grade	1	2.6
Hematopoietic system	Systemic	Large granular lymphocyte leukemia	2	5.1
	Thymus	Thymoma, benign	4	10.3
Digestive system	Glandular stomach	Hemangioma	1	2.6
	Small intestine	Leiomyosarcoma	1	2.6
Endocrine system	Pituitary, pars distalis	Adenoma	12	30.8
	pars intermedia	Adenoma	1	2.6
	Thyroid gland	Adenoma, C-cell	1	2.6
	Adrenal gland	Pheochromocytoma, benign	4	10.3
	Islets of Langerhans	Adenoma, islet cell	9	23.1
Reproductive system	Testis	Leydig cell tumor, benign	2	5.1
	Prostate	Adenoma	2	5.1
		Adenocarcinoma	1	2.6
	Seminal vesicle	Adenoma	1	2.6
	Preputial gland	Squamous cell carcinoma	1	2.6
Others	Subcutis	Lipoma	1	2.6
		Hemangioma	1	2.6
	Zymbal's gland	Squamous cell papilloma	1	2.6

mors, largely owing to pituitary adenomas in the pars distalis, islet cell adenomas, and pheochromocytomas, which represented 52.1% of all neoplastic lesions. In addition to these neoplasms commonly found in aged rats, one adenoma and two hyperplasias of the intermediate lobe of the pituitary gland were found in this study. Proliferative lesions of the intermediate pituitary are not frequently encountered in rats, but the incidence is higher in the Wistar strain compared to F344 or SD strains[11]. A histological analysis of the adenoma in this study showed a large nest of proliferating cells in the pituitary pars intermedia, compressing the nervous and anterior lobes (Fig. 1H). The tumor mass and intact tissue of the lobe were immunohistochemically positive for α-MSH (Fig. 1H inset) and ACTH (data not shown), whereas the pars distalis was only positive for ACTH, suggesting that tumor cells were derived from the intermediate lobe[12]. In the tumor, enlarged cells with prominent nucleoli and mitoses were frequently observed (Fig. 1I).

A prostate adenocarcinoma was encountered in one rat at the scheduled necropsy. It developed in the ventral prostate, in which variedly-sized, multi-layered and irregularly shaped ductal structures were formed by anaplastic tumor cells with chromophobic nuclei (Fig. 1J). Neoplastic cells accompanied by increased stroma and inflammatory cells had partially invaded the surrounding fat tissue, although distant metastases were not observed. While the Leydig cell tumor is one of the most common findings in aged F344 rats, it was not the case in the RccHan:WIST rats, with an incidence of only 5.1%.

The histopathological findings of non-neoplastic lesions observed in this study are summarized in Table 2. The list contains lesions that are commonly found in aged rats, such as foci of altered hepatocytes (FAH), CPN, and other inflammatory and degenerative changes.

Concerning hyperplastic lesions, numerous lesions were observed in the endocrine organs, such as the pancreatic islet, thyroid C-cells, pituitary pars distalis, and parathyroid. In the cases of hyperplasia of the pituitary pars intermedia, cells with enlarged and increased basophilic cytoplasm were focally increased, although no marked compression of the surrounding tissue was observed (Fig. 2A). Incidence of bile duct hyperplasia (5.1%) was markedly less than that of F344 rats (96.8%)[13].

Alveolar macrophage aggregation in the lung was a non-neoplastic lesion with the highest incidence in this study (89.7%; Table 2, Fig. 2B). It was observed as clusters of foamy macrophages often seen in peripheral alveoli. There was no difference in the incidence of this type of lesion between the intact group (18 in 19) and the vehicle-treated group (17 in 20), suggesting that the aggregation may not have been induced by the vehicle treatment. Common bile duct ectasias, with a diameter of 5 mm or larger, were macroscopically observed in nine animals (23.1%). These dilated ducts were commonly composed of foamy and flattened epithelial cells, but in some animals, densely arranged columnar epithelial cells were prominent. The epithelium had folded to form glandular invaginations in the mucosa where a large number of eosinophils had infiltrated (Fig. 2C). "Harderianization" of the extraorbital lacrimal gland[14, 15] was frequently observed. Grossly visible whitish patches on the surface of the gland corresponded to an area where lobes had partially changed from normal serous acini to mucoserous and/or mucous acini (Fig. 2D) that closely resembled those of the Harderian gland. The size of the affected area depended on the individual; affected areas ranged from 0 to 50.5% of the entire section of the gland.

We examined several non-neoplastic lesions further, focusing on the difference between strains using a set of
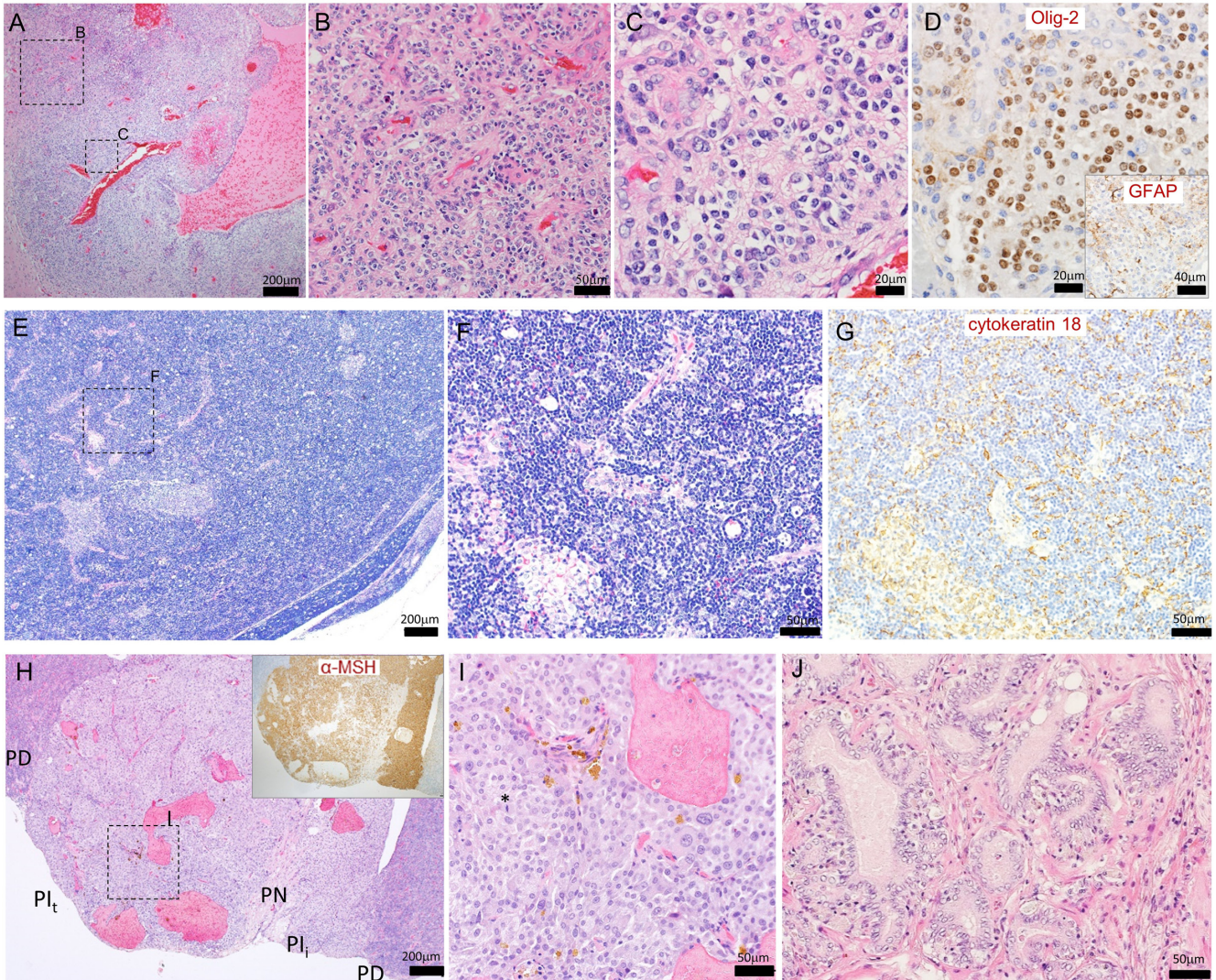
Fig. 1. Histopathological features of neoplasms found in male aged RccHan:WIST rats. A to D: An oligodendroglioma, malignant, high-grade. A: The lesion contained many cysts and capillaries and compressed the normal tissue (lower-left corner). B: The neoplastic cell was pleomorphic and accompanied by atypical endothelial cells. C: Round tumor cells were arranged like a honeycomb structure. D: The immunohistochemical outcomes were positive for Olig-2 and negative for glial fibrillary acidic protein (GFAP) (inset). E to G: Thymoma. A tumor with a cortex/medulla-like structure compressed adjacent thymic tissue. F: A high power view of E. G: The positive immuno-histochemical outcome for cytokeratin 18 is seen in the serial section of F. H and I: A pituitary adenoma of the pars intermedia. H: The tumor mass (PI$_t$) compressed the pars distalis (PD) and the pars nervosa (PN) of the pituitary gland. The intact pars intermedia (PI$_i$) was also observed. The inset shows the positive immunohistochemistry for α-MSH. I: A high-power view of H showing highly pleomorphic cells and a mitotic figure (asterisk). J: A prostate adenocarcinoma. Neoplastic cells formed the glandular structures with marked stromal proliferation.

F344 samples. To obtain quantitative information about FAH, GST-P-positive foci were immunohistochemically analyzed. The number of GST-P positive foci of RccHan:WIST was largely similar to that of F344 rats (Fig. 3A). The GST-P positive area within the liver sections of each animal (Fig. 3B) and the size of each focus (Fig. 3C) were also evaluated, but again, no significant differences were observed. The size of the focus was highly variable depending upon the individual (Fig. 3C).

CPN is one of the most studied non-neoplastic lesions in aged rats. The histological grading of specimens from the two strains we examined demonstrated that the severity of the lesions was much lower in RccHan:WIST than in F344 rats (Table 3). Weber *et al.* reported the lower severity of CPN of RccHan:WIST rats in the comparison with SD rats[16]. It is thus suggested that resistance to spontaneous CPN may be the characteristic of RccHan:WIST.

PCM was detected in 82.4% of rats in this study. The main histological findings for this lesion were focal degeneration of myocardium, mononuclear cell infiltration, and interstitial fibrosis, all of which were frequently observed in the papillary muscle and the area of ventricle close to
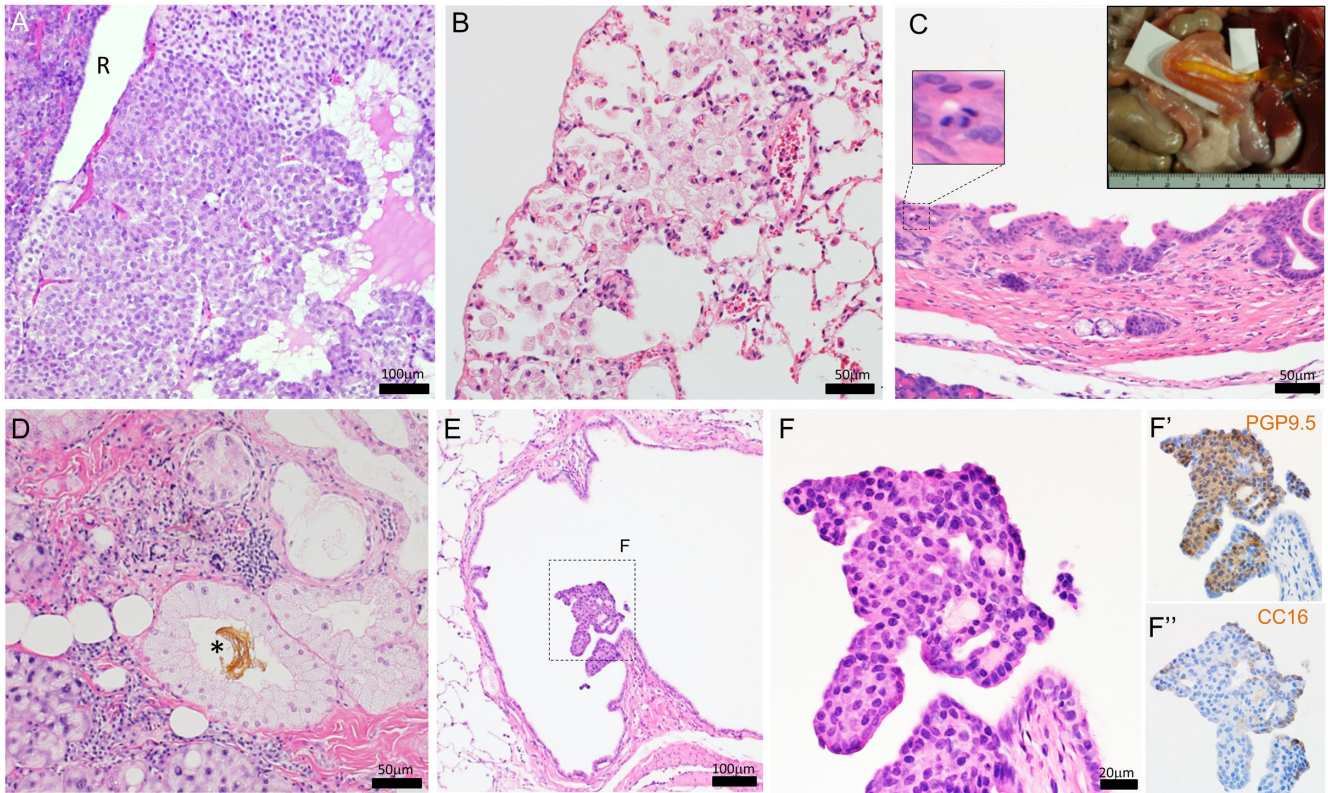
Fig. 2 Histopathological features of non-neoplastic lesions found in aged male RccHan:WIST rats. A: Hyperplasia of the pituitary pars intermedia. Basophilic cells with slightly enlarged nuclei were present near the Rathke's cleft cyst (R). B: Alveolar macrophage aggregation. Foamy cells were densely accumulated through a number of alveoli of the peripheral region. C: Common bile duct ectasia. Epithelia were partially invaginated into the subepithelial connective tissue. High-power view of an occurrence of mitosis is shown in the upper-left corner. The inset shows the gross finding. D: "Harderianization" of the extraorbital lacrimal gland. Large Harderian gland-like acini were localized near degenerative cells with condensed nuclei and an intact lacrimal gland (seen in the lower-left corner). Pigment deposition in an acinar is shown by an asterisk. E: Pulmonary neuroendocrine cell (PNEC) hyperplasia found in the bronchiolar lumen. F: High-power view of E. PNECs had round or oval nuclei with patchy chromatin and are stained with protein G product 9.5 (PGP9.5) (F'). Clara cells with eosinophilic cytoplasm are located at the surface of the mass and stained with CC16 (F'').

the annulus fibrosus. All animals diagnosed with PCM exhibited some extent of fibrous deposition as evidenced by Masson's trichrome staining, and the ratio of the positive area within the section correlated well with the histological grading (data not shown). A histological comparison of PCM between the two strains demonstrated that the severity of the lesions was slightly but significantly lower in the RccHan:WIST rats (Table 4).

Finally, the occurrence of hyperplasia of PNEC in the lung was compared. PNECs are observed as single cells or clusters, called neuroepithelial bodies, in the respiratory epithelium[17]. Although little attention is generally paid to PNECs in the lungs in routine toxicity studies, it is thought that the PNEC has roles in sensing hypoxia and hypercapnia, and PNEC hyperplasia may be associated with chronic inflammation or fibrosis[18–21]. Hyperplasia, defined as a lesion which consists of more than 40 cells[22], was often recognized as a polypoid or a finger-like nodule, protruding into the bronchiolar lumen (Fig. 2E). PNECs had round or oval nuclei with stippled chromatin and vacuolated cytoplasm (Fig. 2F) and were immunohistochemically positive for PGP9.5 (Fig. 2F'). On the surface area of hyperplastic nodules, a few Clara cells, immunohistochemically positive for CC16, were also involved (Fig. 2F''). A histological analysis showed that the incidence of PNEC hyperplasia in aged rats differed between strains, in that Hannover Wistar rats displayed a slightly higher incidence compared to F344 and SD rats[22]. Our results also demonstrated that the incidence of PNEC hyperplasia in RccHan:WIST rats was statistically significantly higher than that in F344 rats (7 out of 39 [17.9%] (Table 2) vs. 0 out of 37 [0%], respectively).

Although the present study was conducted in a small number of animals and only included males, the data contributes to our overall understanding of spontaneous lesions in aged RccHan:WIST rats.

Disclosure of Potential Conflicts of Interest: The authors declare there are no conflicts of interest.

Table 2. Spontaneous Non-neoplastic Lesions Observed in Aged RccHan:WIST Male Rats

Organ syste		Lesion	N	No. of rats with lesions	Rate (%)
Nervous system	Brain	Mineralization, vascular wall	39	1	2.6
		Mineralization, meningeal	39	1	2.6
Hematopoietic system	Bone marrow	Increase of hematopoietic cell	35	6	17.1
		Fibrosis	35	3	8.6
	Thymus	Hyperplasia, epithelial cell	38	2	5.3
		Involution	38	29	76.3
	Spleen	Extramedullary hematopoiesis	39	18	46.2
		Hemosiderosis	39	9	23.1
		Atrophy	39	6	15.4
Cardiovascular system	Heart	Murine progressive cardiomyopathy	34	28	82.4
Respiratory system	Lung	Hyperplasia, pulmonary neuroendocrine cell*	39	7	17.9
		Inflammation	39	20	51.3
		Alveolar macrophage aggregation	39	35	89.7
		Mineralization, vascular wall	39	33	84.6
Digestive system	Glandular stomach	Metaplasia, squamous cell	39	1	2.6
		Edema	39	1	2.6
	Forestomach	Hyperplasia, squamous cell	39	1	2.6
		Ulceration/erosion	39	3	7.7
		Edema	39	1	2.6
	Liver	Foci of cellular alteration, basophilic	38	15	39.5
		Foci of cellular alteration, eosinophilic	38	26	68.4
		Foci of cellular alteration, clear	38	23	60.5
		Vacuolation, hepatocyte	38	4	10.5
		Infiltration of inflammatory cell	38	20	52.6
		Microgranuloma	38	7	18.4
		Bile duct hyperplasia	38	7	18.4
	Pancreas	Hyperplasia, acinar cell	39	1	2.6
		Inflammation	39	5	12.8
		Adipocyte accumulation	39	12	30.8
		Atrophy	39	14	35.9
Endocrine system	Pituitary, pars distalis	Hyperplasia	37	5	13.5
		Cyst/pseudocyst	37	2	5.4
	pars intermedia	Hyperplasia	36	2	5.6
		Cyst/pseudocyst	36	9	25.0
	Adrenal gland	Hyperplasia, cortical, focal	39	4	10.3
		Hyperplasia, medullary, focal	39	5	12.8
		Hyperplasia, medullary, diffuse	39	1	2.6
		Vacuolation, cortical, increased, focal	39	16	41.0
		Vacuolation, cortical, increased, diffuse	39	3	7.7
		Degeneration, cystic	39	1	2.6
		Accessory adrenal	39	5	12.8
	Thyroid gland	Hyperplasia, C-cell	36	11	30.6
	Parathyroid gland	Hyperplasia	25	8	32.0
	Islets of Langerhans	Hyperplasia	39	25	64.1
Urinary system	Kidney	Chronic progressive nephropathy	34	12	35.3
		Mineralization, pelvis	39	6	15.4
		Pelvic inflammation	39	17	43.6
	Bladder	Hyperplasia, urothelium	37	2	5.4
		Inflammation	37	1	2.7
Reproductive system	Testis	Hyperplasia, interstitial cell	39	1	2.6
		Atrophy, seminiferous tubule	39	4	10.3
		Atrophy, interstitial cell	39	1	2.6
	Epididymis	Vacuolation, epithelial	39	9	23.1
		Atrophy	39	2	5.1
	Prostate	Hyperplasia	39	3	7.7
		Inflammation	39	9	23.1
		Concretion	39	33	84.6
		Atrophy	39	23	59.0

Table 2. Continued

Organ syste		Lesion	N	No. of rats with lesions	Rate (%)
	Seminal vesicle	Hyperplasia	36	6	16.7
		Atrophy	36	2	5.6
	Preputial gland	Inflammation/abscess	32	9	28.1
Others	Mammary gland	Hyperplasia	36	2	5.6
		Dilatation, duct/alveolus	36	8	22.2
		Atrophy	36	3	8.3
	Zymbal's gland	Hyperplasia	31	1	3.2
		Ductal ectasia	31	3	9.7
	Harderian gland	Hyperplasia	38	2	5.3
		Inflammation	38	2	5.3
	Extraorbital lacrimal gland	Infiltration of inflammatory cell	38	14	36.8
		"Harderianization"	38	25	65.8
	Eye	Mineralization of cornea	38	4	10.5
	Bone	Hyperosteosis	35	1	2.9

*evaluated by immunohistochemistry using an anti-PGP9.5 antibody.
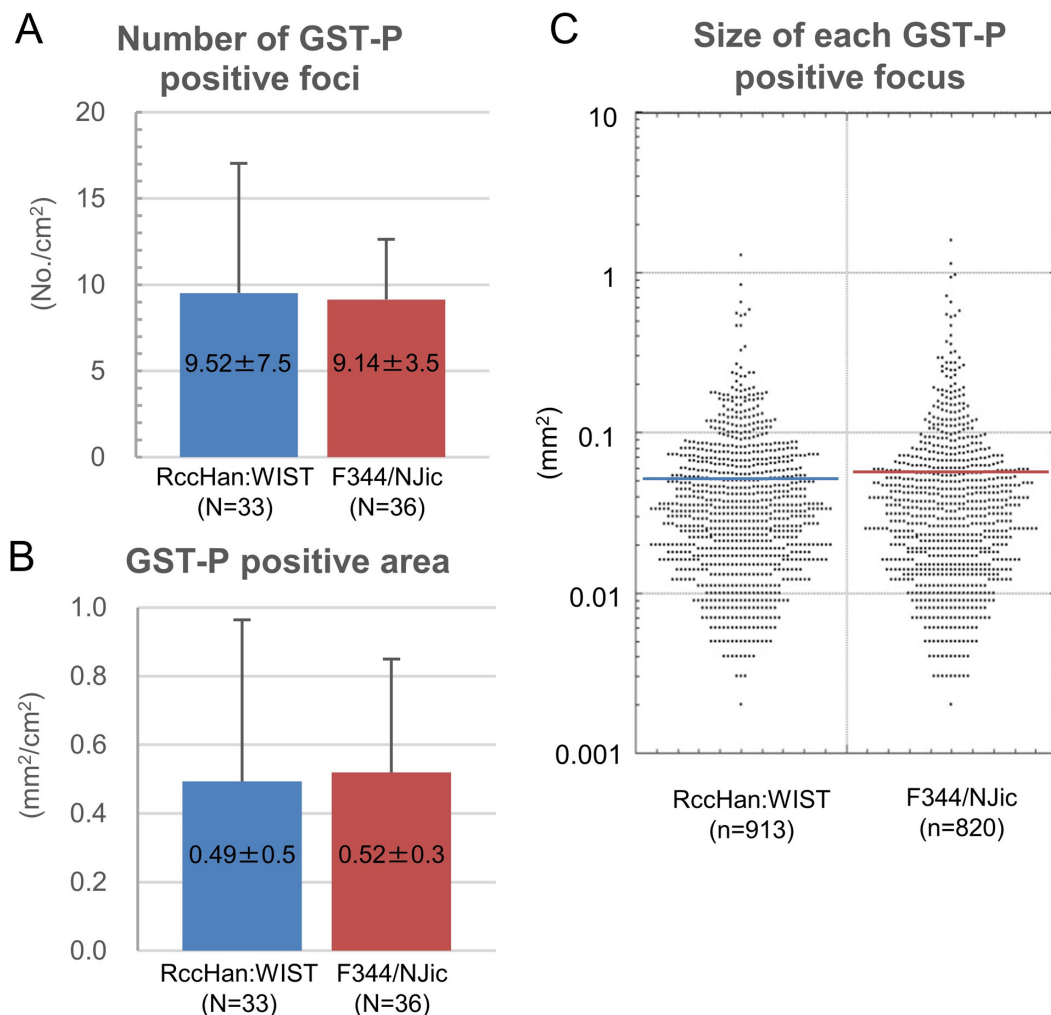
Fig. 3 Comparative analysis of placental glutathione S-transferase (GST-P) positive foci in the liver of aged RccHan:WIST and F344/NJic rats. A: Average number of GST-P positive foci in the liver section (± SD). B: Average GST-P positive area within the liver section (± SD) C: Size distribution of foci which were collected from all examined animals. Each colored bar shows mean value. In all of these comparisons, 33 RccHan:WIST and 36 F344/NJic rats were analyzed, and no significant changes were detected in any of them.

Table 3. Comparison of the Grade of CPN Between Male RccHan:WIST and F344/NJic

Grade	RccHan:WIST (N=34)		F344/NJic (N=37)	
	No. of rats	Rate (%)	No. of rats	Rate (%)
0	17	50.0	0	0
1	5	14.7	0	0
2	5	14.7	1	2.7
3	4	11.8	2	5.4
4	2	5.9	7	18.9
5	1	2.9	9	24.3
6	0	0	12	32.4
7	0	0	4	10.8
8	0	0	2	5.4
Mean grade*	1.2		5.3	

0, no; 1, minimal; 2, mild; 3, low-moderate; 4, mid-moderate; 5, high-moderate; 6, low-severe; 7, high-severe; 8, end-stage. *Significantly different between the strains (Mann Whitney's U test).

Table 4. Comparison of the Grade of PCM Between Male RccHan:WIST and F344/NJic

Grade	RccHan:WIST (N=34)		F344/NJic (N=37)	
	No. of rats	Rate (%)	No. of rats	Rate (%)
0	6	17.6	0	0
1	21	61.8	21	56.8
2	4	11.8	12	32.4
3	3	8.8	3	8.1
4	0	0	1	2.7
Mean grade*	1.1		1.6	

0, absent; 1, minimal; 2, mild; 3, moderate; 4, marked. *Significantly different between the strains (Mann Whitney's U test).

References

1. Envigo. RCCHan:WIST background data. 2016, from Envigo website: http://www.envigo.com/products-services/research-models-services/models/rcchanwist-background-data/.
2. Weber K. Differences in Types and Incidence of Neoplasms in Wistar Han and Sprague-Dawley Rats. Toxicol Pathol. **45**: 64–75. 2017. [Medline][CrossRef]
3. Okamura T, Suzuki S, Ogawa T, Kobayashi J, Kusuoka O, Hatayama K, Mochizuki M, Hoshiya T, Okazaki S, and Tamura K. Background Data for General Toxicology Parameters in RccHan:WIST Rats at 8, 10, 19 and 32 Weeks of Age. J Toxicol Pathol. **24**: 195–205. 2011. [Medline][CrossRef]
4. Hashimoto S, Doi T, Wako Y, Sato J, Wada S, and Tsuchitani M. Corneal mineralization in wistar hannover rats. J Toxicol Pathol. **26**: 275–281. 2013. [Medline][CrossRef]
5. Shimotsuma Y, Takeda S, Ogata K, and Miyata K. Segmen-

tal aplasia of a uterine horn in two RccHan:WIST rats. J Toxicol Pathol. **32**: 293–296. 2019. [Medline][CrossRef]
6. Blankenship B, Eighmy JJ, Hoffmann G, Schroeder M, Sharma AK, and Sorden SD. Findings in Historical Control Harlan RCCHan™: WIST Rats from 104-week Oral Gavage Studies. Toxicol Pathol. **44**: 947–961. 2016. [Medline][CrossRef]
7. Hard GC, and Khan KN. A contemporary overview of chronic progressive nephropathy in the laboratory rat, and its significance for human risk assessment. Toxicol Pathol. **32**: 171–180. 2004. [Medline][CrossRef]
8. Jokinen MP, Lieuallen WG, Boyle MC, Johnson CL, Malarkey DE, and Nyska A. Morphologic aspects of rodent cardiotoxicity in a retrospective evaluation of National Toxicology Program studies. Toxicol Pathol. **39**: 850–860. 2011. [Medline][CrossRef]
9. Weber K, Garman RH, Germann PG, Hardisty JF, Krinke G, Millar P, and Pardo ID. Classification of neural tumors in laboratory rodents, emphasizing the rat. Toxicol Pathol. **39**: 129–151. 2011. [Medline][CrossRef]
10. Tomonari Y, Sato J, Kurotaki T, Wako Y, Kanno T, and Tsuchitani M. Thymomas and Associated Hyperplastic Lesions in Wistar Hannover Rats. Toxicol Pathol. **47**: 129–137. 2019. [Medline][CrossRef]
11. Isobe K, Baily J, Mukaratirwa S, Petterino C, and Bradley A. Historical control background incidence of spontaneous pituitary gland lesions of Han-Wistar and Sprague-Dawley rats and CD-1 mice used in 104-week carcinogenicity stud-

ies. J Toxicol Pathol. **30**: 339–344. 2017. [Medline][Cross-Ref]

12. Oishi Y, Matsumoto M, Yoshizawa K, and Fujihira S. Spontaenous pituitary adenomas of the pars intermedia in mice and rats: histopathological and immunocytochemical studies. J Toxicol Pathol. **5**: 223–231. 1992.[CrossRef]

13. Iwata H, Hirouchi Y, Koike Y, Yamakawa S, Kobayashi K, Yamamoto T, Kobayashi K, Inoue H, and Enomoto M. Historical control data of nonneoplastic and neoplastic lesions in F344/DuCrj rats. J Toxicol Pathol. **4**: 1–24. 1991.[CrossRef]

14. Walker R. Age changes in the rat's exorbital lacrimal gland. Anat Rec. **132**: 49–69. 1958. [Medline][CrossRef]

15. Sashima M, Hatakeyama S, Satoh M, and Suzuki A. Harderianization is another sexual dimorphism of rat exorbital lacrimal gland. Acta Anat (Basel). **135**: 303–306. 1989. [Medline][CrossRef]

16. Weber K, Razinger T, Hardisty JF, Mann P, Martel KC, Frische EA, Blumbach K, Hillen S, Song S, Anzai T, and Chevalier HJ. Differences in rat models used in routine toxicity studies. Int J Toxicol. **30**: 162–173. 2011. [Medline][CrossRef]

17. Gould VE, Linnoila RI, Memoli VA, and Warren WH. Neuroendocrine components of the bronchopulmonary tract: hyperplasias, dysplasias, and neoplasms. Lab Invest. **49**: 519–537. 1983. [Medline]

18. Youngson C, Nurse C, Yeger H, and Cutz E. Oxygen sensing in airway chemoreceptors. Nature. **365**: 153–155. 1993. [Medline][CrossRef]

19. Aguayo SM, Miller YE, Waldron JA Jr, Bogin RM, Sunday ME, Staton GW Jr, Beam WR, and King TE Jr. Brief report: idiopathic diffuse hyperplasia of pulmonary neuroendocrine cells and airways disease. N Engl J Med. **327**: 1285–1288. 1992. [Medline][CrossRef]

20. Gosney J, Heath D, Smith P, Harris P, and Yacoub M. Pulmonary endocrine cells in pulmonary arterial disease. Arch Pathol Lab Med. **113**: 337–341. 1989. [Medline]

21. Elizegi E, Pino I, Vicent S, Blanco D, Saffiotti U, and Montuenga LM. Hyperplasia of alveolar neuroendocrine cells in rat lung carcinogenesis by silica with selective expression of proadrenomedullin-derived peptides and amidating enzymes. Lab Invest. **81**: 1627–1638. 2001. [Medline][Cross-Ref]

22. Haworth R, Woodfine J, McCawley S, Pilling AM, Lewis DJ, and Williams TC. Pulmonary neuroendocrine cell hyperplasia: identification, diagnostic criteria and incidence in untreated ageing rats of different strains. Toxicol Pathol. **35**: 735–740. 2007. [Medline][CrossRef]